Higher Order Multiphase Image Segmentation and Registration

Stephen Keeling
Institute for Mathematics and Scientific Computing
Karl Franzens University of Graz, Austria

in cooperation with
Stefan Fürtinger and Renier Mendoza

Mathematical Image Processing Section, GAMM 2012, Darmstadt

March 28, 2012

Higher Order Models: Total Generalized Variation

Goal: Overcome the essentially piecewise constant model of TV regularization.

Higher Order Models: Total Generalized Variation

Goal: Overcome the essentially piecewise constant model of TV regularization. In the classical approach, minimize:

$$J(I) = \int_{\Omega} |I - \tilde{I}|^2 + \mathrm{TV}_{\alpha}(I)$$

Higher Order Models: Total Generalized Variation

Goal: Overcome the essentially piecewise constant model of TV regularization. In the classical approach, minimize:

$$J(I) = \int_\Omega |I - \tilde{I}|^2 + \mathrm{TV}_\alpha(I) \qquad \text{where}$$

$$\alpha \int_\Omega |DI| = \mathrm{TV}_\alpha(I) = \sup \left\{ \int_\Omega I \, \mathrm{div}\, \boldsymbol{\psi} : \|\boldsymbol{\psi}\|_\infty \leq \alpha, \boldsymbol{\psi} \in C_0^1(\Omega, \mathbb{R}^n) \right\}$$

Higher Order Models: Total Generalized Variation

Goal: Overcome the essentially piecewise constant model of TV regularization. In the classical approach, minimize:

$$J(I) = \int_\Omega |I - \tilde{I}|^2 + \mathrm{TV}_\alpha(I) \qquad \text{where}$$

$$\alpha \int_\Omega |DI| = \mathrm{TV}_\alpha(I) = \sup \left\{ \int_\Omega I \,\mathrm{div}\, \psi : \|\psi\|_\infty \leq \alpha, \psi \in C_0^1(\Omega, \mathbb{R}^n) \right\}$$

Noisy and TV-reconstructed images:

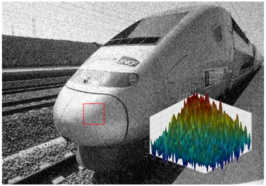

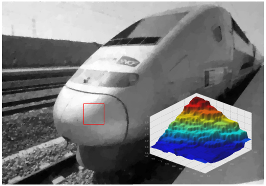

Higher Order Models: Total Generalized Variation

Goal: Develop a functional with a kernel which is richer than piecewise constants.

Higher Order Models: Total Generalized Variation

Goal: Develop a functional with a kernel which is richer than piecewise constants. In the generalized approach, minimize:

$$J(I) = \int_\Omega |I - \tilde{I}|^2 + \mathrm{TGV}_\alpha^k(I)$$

Higher Order Models: Total Generalized Variation

Goal: Develop a functional with a kernel which is richer than piecewise constants. In the generalized approach, minimize:

$$J(I) = \int_\Omega |I - \tilde{I}|^2 + \mathrm{TGV}_{\boldsymbol{\alpha}}^k(I) \qquad \text{where}$$

$$\mathrm{TGV}_{\boldsymbol{\alpha}}^k(I) = \sup \left\{ \int_\Omega I \,\mathrm{div}^k \boldsymbol{\psi} : \underbrace{\|\mathrm{div}^l \boldsymbol{\psi}\|_\infty \leq \alpha_l}_{l=0,\dots,k-1}, \boldsymbol{\psi} \in C_0^k(\Omega, \mathrm{Sym}^k(\mathbb{R}^n)) \right\}$$

Higher Order Models: Total Generalized Variation

Goal: Develop a functional with a kernel which is richer than piecewise constants. In the generalized approach, minimize:

$$J(I) = \int_\Omega |I - \tilde{I}|^2 + \mathrm{TGV}_{\alpha}^{k}(I) \qquad \text{where}$$

$$\mathrm{TGV}_{\alpha}^{k}(I) = \sup\left\{ \int_\Omega I \,\mathrm{div}^k \psi : \underbrace{\|\mathrm{div}^l \psi\|_\infty \leq \alpha_l}_{l=0,\ldots,k-1}, \psi \in C_0^k(\Omega, \mathrm{Sym}^k(\mathbb{R}^n)) \right\}$$

Noisy and $\mathrm{TGV}_{\alpha}^{2}$-reconstructed images: [Bredies, Kunisch, Pock]

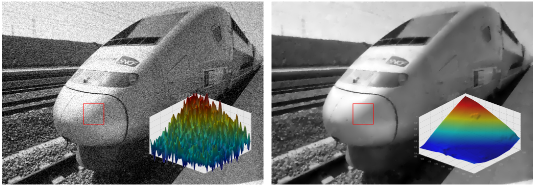

Higher Order Models: Total Generalized Variation

Note: For example, $\mathrm{TGV}_{\boldsymbol{\alpha}}^2$ reformulated with duality as

$$\mathrm{TGV}_{\boldsymbol{\alpha}}^2(I) = \min_{\boldsymbol{G}} \int_\Omega \left\{ \alpha_1 |DI - \boldsymbol{G}| + \tfrac{1}{2}\alpha_1 |\nabla \boldsymbol{G}^{\mathrm{T}} + \nabla \boldsymbol{G}| \right\}$$

Higher Order Models: Total Generalized Variation

Note: For example, $\mathrm{TGV}_{\boldsymbol{\alpha}}^2$ reformulated with duality as

$$\mathrm{TGV}_{\boldsymbol{\alpha}}^2(I) = \min_{\boldsymbol{G}} \int_{\Omega} \left\{ \alpha_1 |DI - \boldsymbol{G}| + \tfrac{1}{2}\alpha_1 |\nabla \boldsymbol{G}^{\mathrm{T}} + \nabla \boldsymbol{G}| \right\}$$

Locally:

- DI smooth $\Rightarrow \boldsymbol{G} = \nabla I \approx$ optimal $\Rightarrow \mathrm{TGV}_{\boldsymbol{\alpha}}^2(I) \approx \alpha_0 \int_{\mathrm{loc}} |\nabla^2 I|$.
- I jumps $\Rightarrow \boldsymbol{G} = 0 \approx$ optimal $\Rightarrow \mathrm{TGV}_{\boldsymbol{\alpha}}^2(I) \approx \alpha_1 \int_{\mathrm{loc}} |\nabla I|$.

Higher Order Models: Total Generalized Variation

Note: For example, $\mathrm{TGV}_{\alpha}^{2}$ reformulated with duality as

$$\mathrm{TGV}_{\alpha}^{2}(I) = \min_{\boldsymbol{G}} \int_{\Omega} \left\{ \alpha_1 |DI - \boldsymbol{G}| + \tfrac{1}{2}\alpha_1 |\nabla \boldsymbol{G}^{\mathrm{T}} + \nabla \boldsymbol{G}| \right\}$$

Locally:

- DI smooth $\Rightarrow \boldsymbol{G} = \nabla I \approx$ optimal $\Rightarrow \mathrm{TGV}_{\alpha}^{2}(I) \approx \alpha_0 \int_{\mathrm{loc}} |\nabla^2 I|$.
- I jumps $\Rightarrow \boldsymbol{G} = 0 \approx$ optimal $\Rightarrow \mathrm{TGV}_{\alpha}^{2}(I) \approx \alpha_1 \int_{\mathrm{loc}} |\nabla I|$.

Generally:

- So computing $\mathrm{TGV}_{\alpha}^{2}$ can be seen as solving a minimization problem,
- in which terms of first and second order are optimally balanced out,
- and the vector field $\boldsymbol{G}$ represents the smooth part of the measure DI.

Higer Order Models for Segmentation and Registration

Example:

Objective: Remove the motion in a DCE-MRI sequence so that individual tissue points can be investigated.

Higer Order Models for Segmentation and Registration

Example:

Objective: Remove the motion in a DCE-MRI sequence so that individual tissue points can be investigated.

Challenges: Contrast changes with time, and the images are far from piecewise constant.

Higer Order Models for Segmentation and Registration

Example:

Objective: Remove the motion in a DCE-MRI sequence so that individual tissue points can be investigated.

Challenges: Contrast changes with time, and the images are far from piecewise constant.

Plan: Segment the images, transform the edge sets to diffuse surfaces using blurring, register the diffuse surfaces with progressively less blurring.

Established Approaches to Segmentation

Method of kmeans:

$$\min_{p_k,\chi_k}\left\{\sum_{k=1}^{K}\int_\Omega |p_k\chi_k-\tilde{I}|^2 : \{p_k\}\in\mathcal{P}^0, \chi_k:\Omega\to\{0,1\}\right\}$$

Established Approaches to Segmentation

Method of kmeans:

$$\min_{p_k,\chi_k}\left\{\sum_{k=1}^{K}\int_\Omega |p_k\chi_k-\tilde{I}|^2 : \{p_k\}\in\mathcal{P}^0, \chi_k:\Omega\to\{0,1\}\right\}$$

Minimizing the Mumford-Shah functional:

$$\min_{I,\Gamma}\left\{\int_\Omega |I-\tilde{I}|^2+\delta^{-1}\int_{\Omega\setminus\Gamma}|\nabla I|^2+\beta|\Gamma|\right\}$$

Established Approaches to Segmentation

Method of kmeans:

$$\min_{p_k,\chi_k} \left\{ \sum_{k=1}^{K} \int_\Omega |p_k \chi_k - \tilde{I}|^2 : \{p_k\} \in \mathcal{P}^0, \chi_k : \Omega \to \{0,1\} \right\}$$

Minimizing the Mumford-Shah functional:

$$\min_{I,\Gamma} \left\{ \int_\Omega |I - \tilde{I}|^2 + \delta^{-1} \int_{\Omega \setminus \Gamma} |\nabla I|^2 + \beta |\Gamma| \right\}$$

or the Ambrosio-Tortorelli phase function approximation:

$$\min_{I,\chi} \left\{ \int_\Omega \left[|I - \tilde{I}|^2 + \delta^{-1} |\nabla I|^2 \chi^2 + \epsilon |\nabla \chi|^2 + \epsilon^{-1} |1 - \chi|^2 \right] \right\}$$

Higher Order Counterparts

Method of kmeans:

$$\min_{p_k,\chi_k} \left\{ \sum_{m=1}^{M} \int_\Omega |p_k \chi_k - \tilde{I}|^2 : \{p_k\} \in \mathcal{P}^{m-1}, \chi_k : \Omega \to \{0,1\} \right\}$$

Minimizing the Mumford-Shah functional:

$$\min_{I,\Gamma} \left\{ \int_\Omega |I - \tilde{I}|^2 + \delta^{-1} \int_{\Omega \setminus \Gamma} |\nabla^m I|^2 + \beta |\Gamma| \right\}$$

or the Ambrosio-Tortorelli phase function approximation:

$$\min_{I,\chi} \left\{ \int_\Omega \left[|I - \tilde{I}|^2 + \delta^{-1} |\nabla^m I|^2 \chi^2 + \epsilon |\nabla \chi|^2 + \epsilon^{-1} |1 - \chi|^2 \right] \right\}$$

Representative Problems with These Methods

kmeans leads to staircasing and disconnectedness:

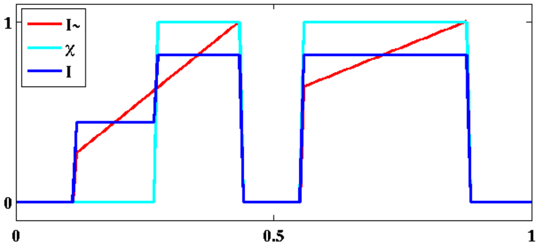

Representative Problems with These Methods

kmeans leads to staircasing and disconnectedness:

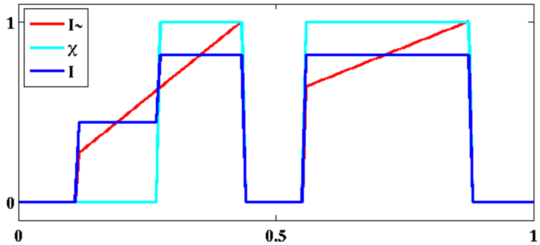

Ambrosio-Tortorelli gives a *fuzzy* edge function:

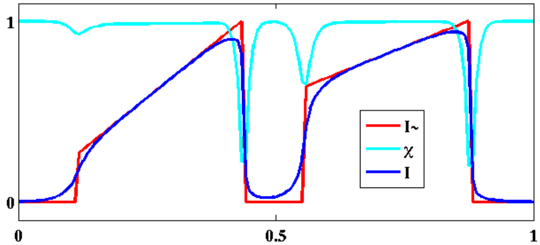

Higher Order on Connected Components of Segments

Constant

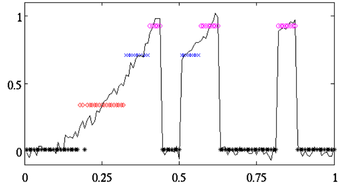

Linear

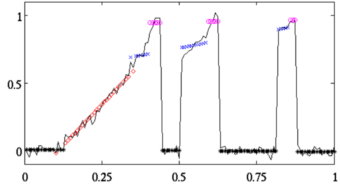

Quadratic

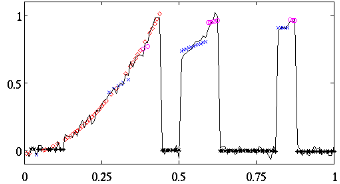

Higher Order on Connected Components of Segments

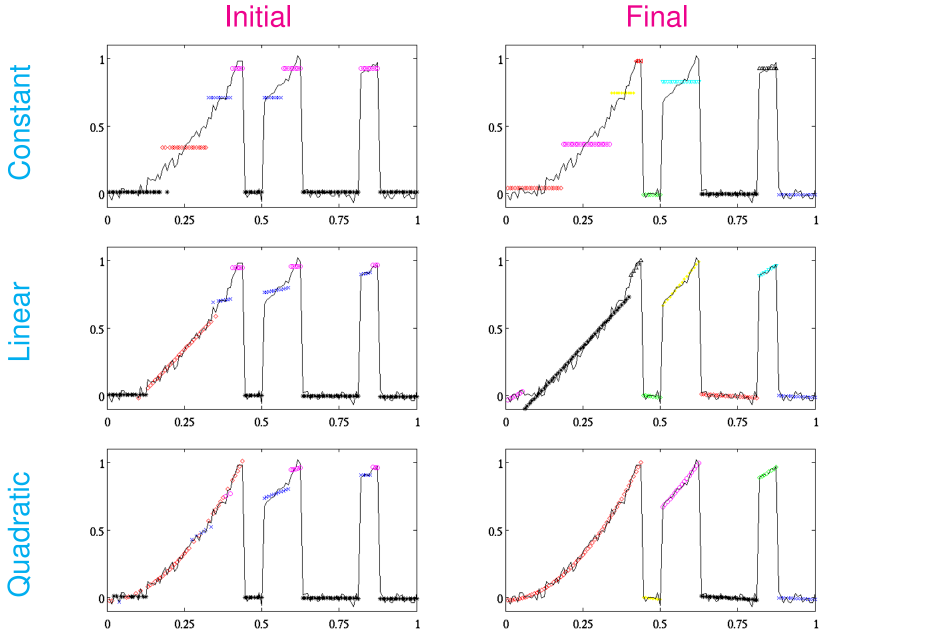

Proposed Multiphase Segmentation Approach

Use multiple phase functions $\{\chi_k\}$ and model functions $\{I_k\}$.

Estimate $\tilde{I} \approx \sum_{k=1}^{K} I_k \chi_k$

Proposed Multiphase Segmentation Approach

Use multiple phase functions $\{\chi_k\}$ and model functions $\{I_k\}$.

Estimate $\tilde{I} \approx \sum_{k=1}^{K} I_k \chi_k$ through minimizing:

$$\min_{\{I_k\},\{\chi_k\}} \left\{ \sum_{k=1}^{K} \int_\Omega \left[|I_k - \tilde{I}|^2 {\chi_k}^2 + (\epsilon + \epsilon^{-1} {\chi_k}^2) |\nabla^m I_k|^2 \right. \right.$$

Proposed Multiphase Segmentation Approach

Use multiple phase functions $\{\chi_k\}$ and model functions $\{I_k\}$.

Estimate $\tilde{I} \approx \sum_{k=1}^{K} I_k \chi_k$ through minimizing:

$$\min_{\{I_k\},\{\chi_k\}} \left\{ \sum_{k=1}^{K} \int_{\Omega} \left[|I_k - \tilde{I}|^2 {\chi_k}^2 + (\epsilon + \epsilon^{-1} {\chi_k}^2) |\nabla^m I_k|^2 \right. \right.$$

$$\left. \left. + \delta |\nabla \chi_k|^2 + \delta^{-1} |\chi_k (\chi_k - 1)|^2 \right] + \delta^{-1} \int_{\Omega} \left[\sum_{l=1}^{K} \chi_l - 1 \right]^2 \right\}$$

Proposed Multiphase Segmentation Approach

Use multiple phase functions $\{\chi_k\}$ and model functions $\{I_k\}$.

Estimate $\tilde{I} \approx \sum_{k=1}^{K} I_k \chi_k$ through minimizing:

$$\min_{\{I_k\},\{\chi_k\}} \left\{ \sum_{k=1}^{K} \int_\Omega \left[|I_k - \tilde{I}|^2 {\chi_k}^2 + (\epsilon + \epsilon^{-1} {\chi_k}^2) |\nabla^m I_k|^2 \right. \right.$$

$$\left. \left. + \delta |\nabla \chi_k|^2 + \delta^{-1} |\chi_k(\chi_k - 1)|^2 \right] + \delta^{-1} \int_\Omega \left[\sum_{l=1}^{K} \chi_l - 1 \right]^2 \right\}$$

Combines elements of kmeans and Ambrosio Tortorelli.

Proposed Multiphase Segmentation Approach

Simplification:

$$\min_{\{I_k\}} \sum_{k=1}^{K} \int_\Omega \left[|I_k - \tilde{I}|^2 \chi_k + (\epsilon + \epsilon^{-1}\chi_k)|\nabla^m I_k|^2 \right]$$

with each χ_k binary and depending upon $\{I_l\}$:

$$\chi_k(\boldsymbol{x}) = \begin{cases} 1, & |I_k(\boldsymbol{x}) - \tilde{I}(\boldsymbol{x})| < |I_l(\boldsymbol{x}) - \tilde{I}(\boldsymbol{x})|, \quad \forall l \neq k \\ 0, & \text{otherwise.} \end{cases}$$

Proposed Multiphase Segmentation Approach

Simplification:

$$\min_{\{I_k\}} \sum_{k=1}^{K} \int_\Omega \left[|I_k - \tilde{I}|^2 \chi_k + (\epsilon + \epsilon^{-1}\chi_k)|\nabla^m I_k|^2 \right]$$

with each χ_k binary and depending upon $\{I_l\}$:

$$\chi_k(\boldsymbol{x}) = \begin{cases} 1, & |I_k(\boldsymbol{x}) - \tilde{I}(\boldsymbol{x})| < |I_l(\boldsymbol{x}) - \tilde{I}(\boldsymbol{x})|, \quad \forall l \neq k \\ 0, & \text{otherwise.} \end{cases}$$

Effects:

- $\epsilon^{-1}\chi_k|\nabla^m I_k|^2 \Rightarrow I_k$ nearly in $\mathcal{P}^{m-1}$ on each connected component of $(\chi_k = 1)$.

Proposed Multiphase Segmentation Approach

Simplification:

$$\min_{\{I_k\}} \sum_{k=1}^{K} \int_\Omega \left[|I_k - \tilde{I}|^2 \chi_k + (\epsilon + \epsilon^{-1}\chi_k) |\nabla^m I_k|^2 \right]$$

with each χ_k binary and depending upon $\{I_l\}$:

$$\chi_k(\boldsymbol{x}) = \begin{cases} 1, & |I_k(\boldsymbol{x}) - \tilde{I}(\boldsymbol{x})| < |I_l(\boldsymbol{x}) - \tilde{I}(\boldsymbol{x})|, \quad \forall l \neq k \\ 0, & \text{otherwise.} \end{cases}$$

Effects:

- $\epsilon^{-1}\chi_k |\nabla^m I_k|^2 \Rightarrow I_k$ nearly in $\mathcal{P}^{m-1}$ on each connected component of $(\chi_k = 1)$.
- $\epsilon |\nabla^m I_k|^2 \Rightarrow I_k$ extended naturally outside $(\chi_k = 1)$.

Proposed Multiphase Segmentation Approach

Simplification:

$$\min_{\{I_k\}} \sum_{k=1}^{K} \int_\Omega \left[|I_k - \tilde{I}|^2 \chi_k + (\epsilon + \epsilon^{-1}\chi_k)|\nabla^m I_k|^2 \right]$$

with each χ_k binary and depending upon $\{I_l\}$:

$$\chi_k(\boldsymbol{x}) = \begin{cases} 1, & |I_k(\boldsymbol{x}) - \tilde{I}(\boldsymbol{x})| < |I_l(\boldsymbol{x}) - \tilde{I}(\boldsymbol{x})|, \quad \forall l \neq k \\ 0, & \text{otherwise.} \end{cases}$$

Effects:

- $\epsilon^{-1}\chi_k|\nabla^m I_k|^2 \Rightarrow I_k$ nearly in $\mathcal{P}^{m-1}$ on each connected component of $(\chi_k = 1)$.
- $\epsilon|\nabla^m I_k|^2 \Rightarrow I_k$ extended naturally outside $(\chi_k = 1)$.
- $|I_k - \tilde{I}|^2\chi_k \Rightarrow I_k \approx \tilde{I}$ on $(\chi_k = 1)$.

Computational Investigation of the Approach

Example: $K = 2$, $m = 2$, $\{\chi_k\}$ & $\{I_k\}$ by splitting, $\chi = \chi_1$.

Given:

Fig 2a

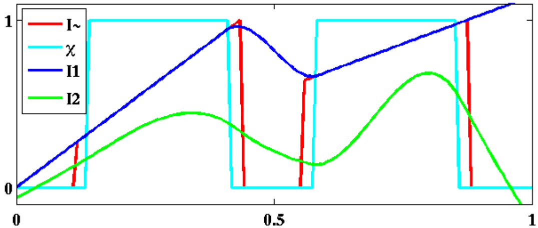

Computational Investigation of the Approach

Example: $K = 2$, $m = 2$, $\{\chi_k\}$ & $\{I_k\}$ by splitting, $\chi = \chi_1$.

Given:

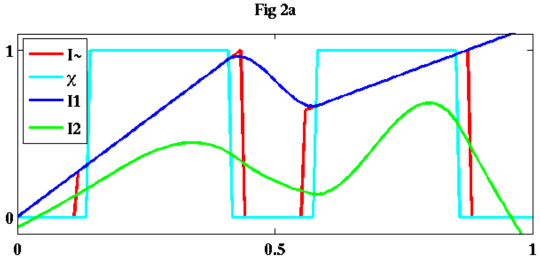

Since $|I_1 - \tilde{I}| < |I_2 - \tilde{I}|$ on and just outside $(\chi = 1)$, next curves:

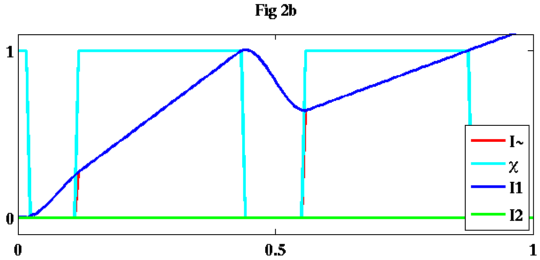

Computational Investigation of the Approach

($\chi = 1$) has grown to include ($\tilde{I} > 0$), but also some ($x < \delta$),

Fig 2b

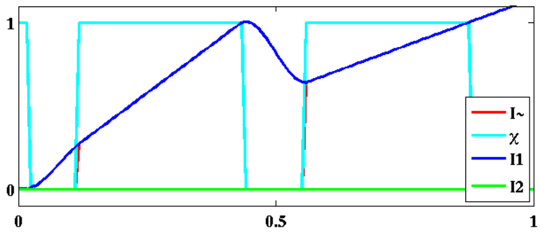

Computational Investigation of the Approach

($\chi = 1$) has grown to include ($\tilde{I} > 0$), but also some ($x < \delta$),

Fig 2b

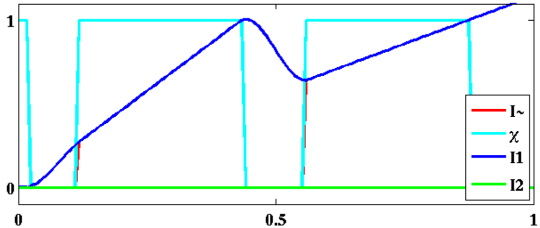

Since $|I_1 - \tilde{I}| < |I_2 - \tilde{I}|$ in ($x < \delta$), converged result:

Fig 2c

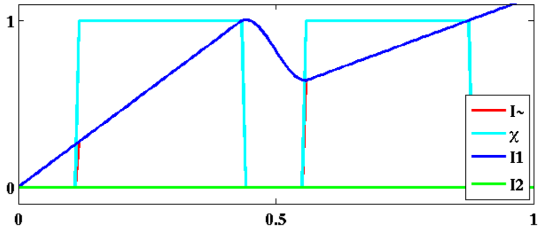

Computational Investigation of the Approach

Converged result:

Fig 2c

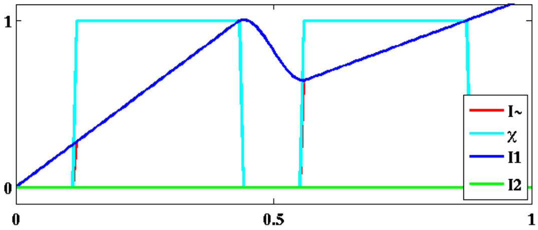

Computational Investigation of the Approach

Converged result:

Fig 2c

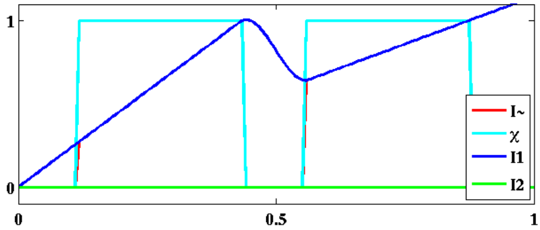

Effects: $(K = 2, m = 2, \chi = \chi_1)$

- $\epsilon^{-1}\chi_k|\nabla^m I_k|^2 \Rightarrow I_k$ nearly in $\mathcal{P}^{m-1}$ on each connected component of $(\chi_k = 1)$.
- $\epsilon|\nabla^m I_k|^2 \Rightarrow I_k$ extended naturally outside $(\chi_k = 1)$.
- $|I_k - \tilde{I}|^2\chi_k \Rightarrow I_k \approx \tilde{I}$ on $(\chi_k = 1)$.

Computational Investigation of the Approach

Above $\tilde{I}$ was piecewise linear, now piecewise quadratic:

Fig 3a

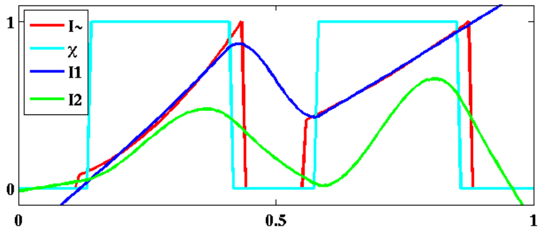

Computational Investigation of the Approach

Above $\tilde{I}$ was piecewise linear, now piecewise quadratic:

Fig 3a

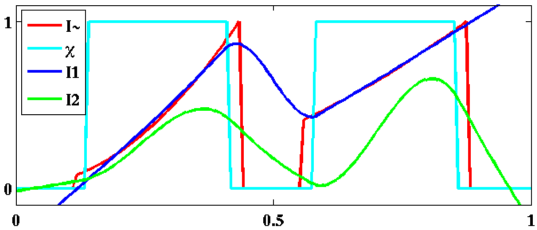

Converged result with an unnatural edge in left piece of ($\tilde{I} > 0$):

Fig 3b

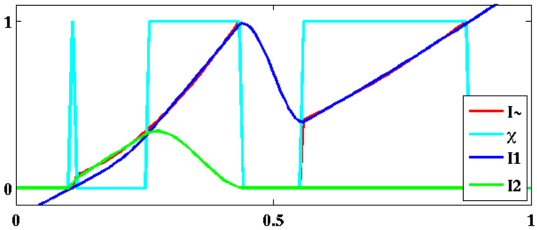

Computational Investigation of the Approach

This result motivates changing $\epsilon^{-1}\chi_k$ to $\alpha\chi_k$ where $\alpha \ll \epsilon^{-1}$ as $\epsilon \to 0$ (small, i.e., ϵ need not be tuned).

New simplified approach:

$$\min_{\{I_k\}} \sum_{k=1}^{K} \int_\Omega \left[|I_k - \tilde{I}|^2 \chi_k + (\epsilon + \alpha\chi_k) |\nabla^m I_k|^2 \right]$$

again with each χ_k binary and depending upon $\{I_l\}$:

$$\chi_k(\boldsymbol{x}) = \begin{cases} 1, & |I_k(\boldsymbol{x}) - \tilde{I}(\boldsymbol{x})| < |I_l(\boldsymbol{x}) - \tilde{I}(\boldsymbol{x})|, \quad \forall l \neq k \\ 0, & \text{otherwise.} \end{cases}$$

Computational Investigation of the Approach

This result motivates changing $\epsilon^{-1}\chi_k$ to $\alpha\chi_k$ where $\alpha \ll \epsilon^{-1}$ as $\epsilon \to 0$ (small, i.e., ϵ need not be tuned).

New simplified approach:

$$\min_{\{I_k\}} \sum_{k=1}^{K} \int_{\Omega} \left[|I_k - \tilde{I}|^2 \chi_k + (\epsilon + \alpha\chi_k) |\nabla^m I_k|^2 \right]$$

again with each χ_k binary and depending upon $\{I_l\}$:

$$\chi_k(\boldsymbol{x}) = \begin{cases} 1, & |I_k(\boldsymbol{x}) - \tilde{I}(\boldsymbol{x})| < |I_l(\boldsymbol{x}) - \tilde{I}(\boldsymbol{x})|, \quad \forall l \neq k \\ 0, & \text{otherwise.} \end{cases}$$

(Alternative to choosing α: Increase the order m.)

Computational Investigation of the Approach

$|I_1 - \tilde{I}|$ small near ($\chi = 1$) and $|I_2 - \tilde{I}|$ large near ($\chi = 0$):

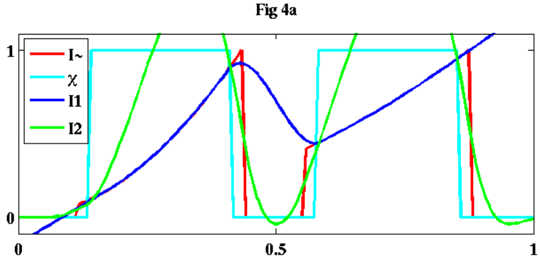

Computational Investigation of the Approach

$|I_1 - \tilde{I}|$ small near ($\chi = 1$) and $|I_2 - \tilde{I}|$ large near ($\chi = 0$):

Fig 4a

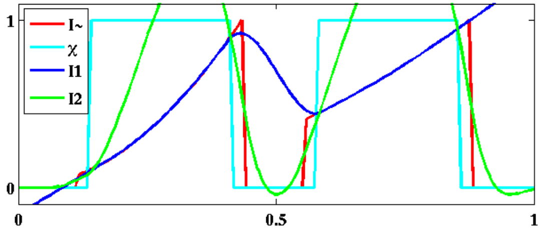

$\alpha < \epsilon^{-1} \Rightarrow |I_1 - \tilde{I}| < |I_2 - \tilde{I}|$ always near ($\chi = 1$). Finally:

Fig 4b

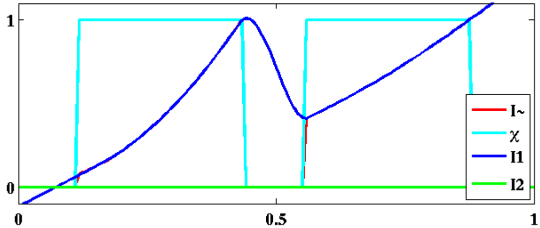

Computational Investigation of the Approach

But the method can still get stuck:

Fig 5

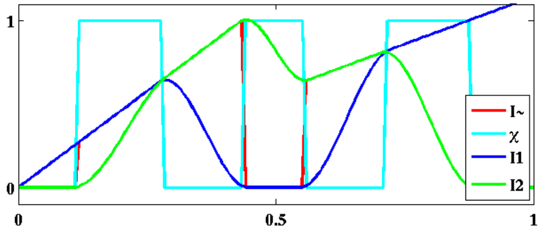

Computational Investigation of the Approach

But the method can still get stuck:

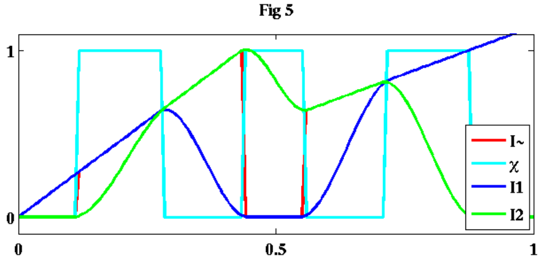

- $\tilde{I}$ is simply piecewise linear.
- $0 \approx |I_1 - \tilde{I}| < |I_2 - \tilde{I}|$ on $(\chi = 1)$.
- $0 \approx |I_2 - \tilde{I}| < |I_1 - \tilde{I}|$ on $(\chi = 0)$.

Computational Investigation of the Approach

But the method can still get stuck:

Fig 5

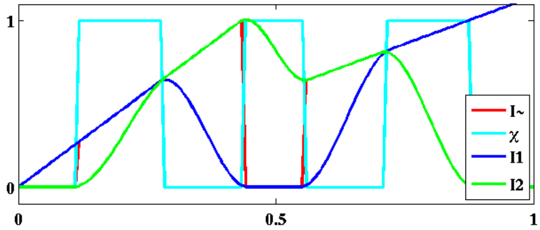

- $\tilde{I}$ is simply piecewise linear.
- $0 \approx |I_1 - \tilde{I}| < |I_2 - \tilde{I}|$ on $(\chi = 1)$.
- $0 \approx |I_2 - \tilde{I}| < |I_1 - \tilde{I}|$ on $(\chi = 0)$.
- Result is converged.

Computational Investigation of the Approach

But the method can still get stuck:

Fig 5

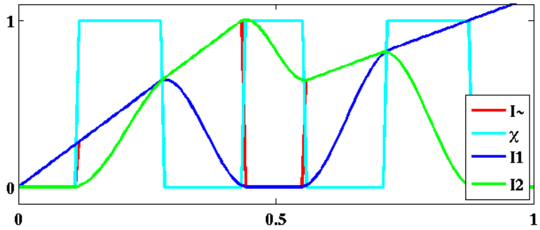

- $\tilde{I}$ is simply piecewise linear.
- $0 \approx |I_1 - \tilde{I}| < |I_2 - \tilde{I}|$ on $(\chi = 1)$.
- $0 \approx |I_2 - \tilde{I}| < |I_1 - \tilde{I}|$ on $(\chi = 0)$.
- Result is converged.
- Such cases are more likely with $K > 2$.

Determining Edges

Examples motivate starting with $\{\chi_k\}$ which respect edges.

Determining Edges

Examples motivate starting with $\{\chi_k\}$ which respect edges.

Determining non-fuzzy edge set $(\chi = 0)$ for $\chi : \Omega \to \{0, 1\}$:

$$\min_{\chi} \int_{\Omega} |I(\chi) - \tilde{I}|^2 \quad \text{where} \quad I(\chi) = \arg\min_{I} \int_{\Omega} \left[|I - \tilde{I}|^2 \chi + (\epsilon + \alpha\chi) |\nabla^m I|^2 \right]$$

Fig 6

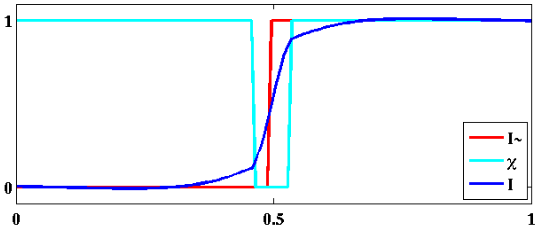

Determining Edges

Examples motivate starting with $\{\chi_k\}$ which respect edges.

Determining non-fuzzy edge set $(\chi = 0)$ for $\chi : \Omega \to \{0, 1\}$:

$$\min_{\chi} \int_{\Omega} |I(\chi) - \tilde{I}|^2 \quad \text{where} \quad I(\chi) = \arg\min_{I} \int_{\Omega} \left[|I - \tilde{I}|^2 \chi + (\epsilon + \alpha\chi) |\nabla^m I|^2 \right]$$

Fig 6

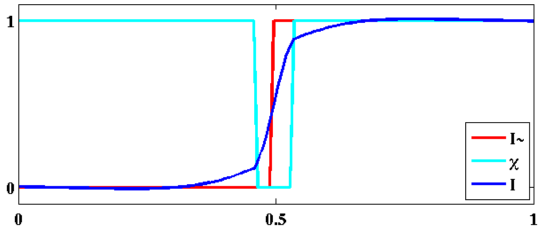

Here the edge set $(\chi = 0) = (|x| < \delta)$ can be determined explicitly by minimizing with respect to δ.

Determining Edges

Examples motivate starting with $\{\chi_k\}$ which respect edges.

Determining non-fuzzy edge set $(\chi = 0)$ for $\chi : \Omega \to \{0, 1\}$:

$$\min_{\chi} \int_{\Omega} |I(\chi) - \tilde{I}|^2 \quad \text{where} \quad I(\chi) = \arg\min_{I} \int_{\Omega} \left[|I - \tilde{I}|^2 \chi + (\epsilon + \alpha\chi) |\nabla^m I|^2 \right]$$

Fig 6

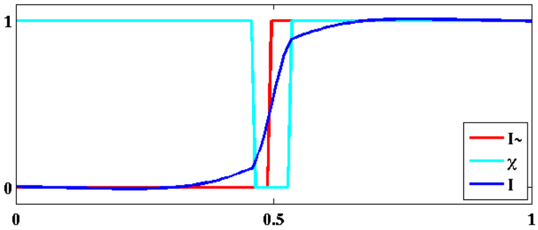

Here the edge set $(\chi = 0) = (|x| < \delta)$ can be determined explicitly by minimizing with respect to δ. In general?...

Edge Determination Approach

Edge set is $(\chi = 0)$ for $\chi : \Omega \to \{0, 1\}$,

$$\chi(\boldsymbol{x}) = \begin{cases} 1, & |I_\mathrm{b}(\boldsymbol{x}) - \tilde{E}(\boldsymbol{x})| < \theta |I_\mathrm{f}(\boldsymbol{x}) - \tilde{E}(\boldsymbol{x})| \\ 0, & \text{otherwise.} \end{cases}$$

Fuzzy edge function $\tilde{E} = |\nabla I_\mathrm{s}|$,

$$I_\mathrm{s} = \arg\min_{I} \int_\Omega \left[|I - \tilde{I}|^2 \chi + (\epsilon + \alpha\chi)|\nabla^m I|^2 \right]$$

I_b and I_f are background and foreground estimations of $\tilde{E}$,

$$I_\mathrm{b} = \arg\min_{I} \int_\Omega \left[|I - \tilde{E}|^2 \chi + (\epsilon + \alpha\chi)|\nabla I|^2 \right]$$

$$I_\mathrm{f} = \arg\min_{I} \int_\Omega \left[|I - \tilde{E}|^2 (1-\chi) + (\epsilon + \alpha(1-\chi))|\nabla I|^2 \right]$$

Edge Determination Approach

Example:

Fig 7

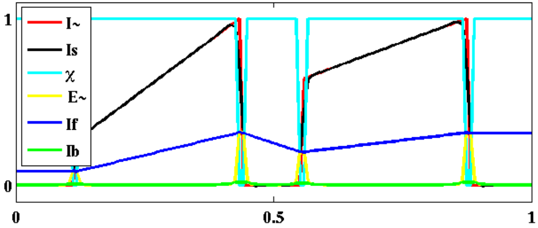

Computed by splitting, starting with $\chi = 1$, then

$$\cdots \to \chi \to I_s \to \tilde{E} \to \{I_f, I_b, \chi\} \to \chi \to \cdots$$

Edge Determination Approach

Example:

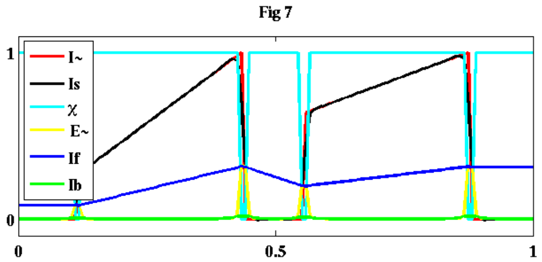

Computed by splitting, starting with $\chi = 1$, then

$$\cdots \to \chi \to I_s \to \tilde{E} \to \{I_f, I_b, \chi\} \to \chi \to \cdots$$

Theorem: There exists a fixed point for this mapping.
[Fürtinger & Keeling]

Segmentation Regularization

Segments are regularized by smoothing $\{\chi_l\}$ according to

$$\psi_l = \arg\min_{\psi} \int_{\Omega} \left[|\psi - \chi_l|^2 + \delta |\nabla \psi|^2 \right], \quad l = 1, \ldots, L$$

and updating

$$\phi(\boldsymbol{x}) = l, \quad \forall \boldsymbol{x} : \chi_l(\boldsymbol{x}) = 1$$

for redefined

$$\chi_l(\boldsymbol{x}) = \begin{cases} 1, & \psi_l(\boldsymbol{x}) > \psi_k(\boldsymbol{x}), \quad \forall k \neq l \\ 0, & \text{otherwise} \end{cases}$$

Segmentation Regularization

Segments are regularized by smoothing $\{\chi_l\}$ according to

$$\psi_l = \arg\min_{\psi} \int_{\Omega} \left[|\psi - \chi_l|^2 + \delta |\nabla \psi|^2 \right], \quad l = 1, \ldots, L$$

and updating

$$\phi(\boldsymbol{x}) = l, \quad \forall \boldsymbol{x} : \chi_l(\boldsymbol{x}) = 1$$

for redefined

$$\chi_l(\boldsymbol{x}) = \begin{cases} 1, & \psi_l(\boldsymbol{x}) > \psi_k(\boldsymbol{x}), \quad \forall k \neq l \\ 0, & \text{otherwise} \end{cases}$$

Resulting segments are smoother with increasing δ.

Computational Investigation of the Approach

2D Examples:

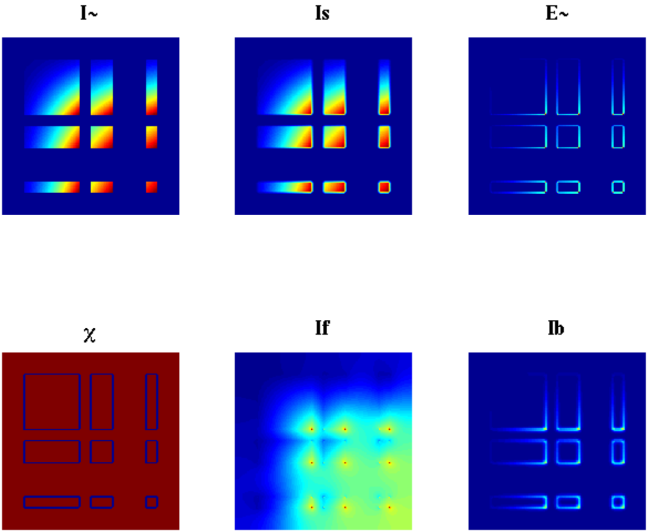

Computational Investigation of the Approach

2D Examples:

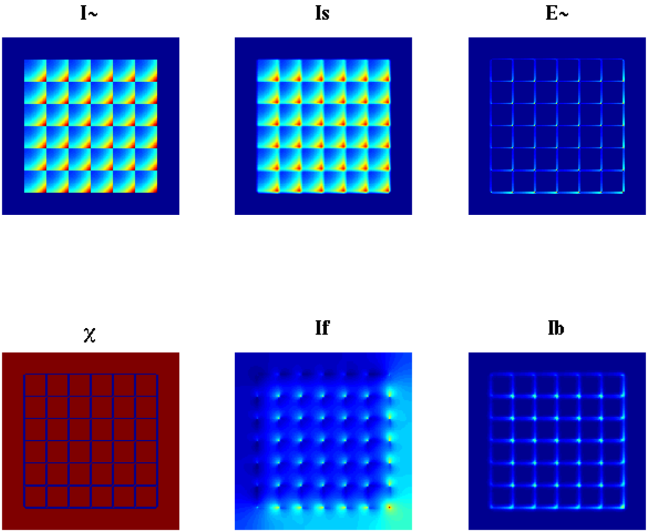

Computational Investigation of the Approach

2D Examples:

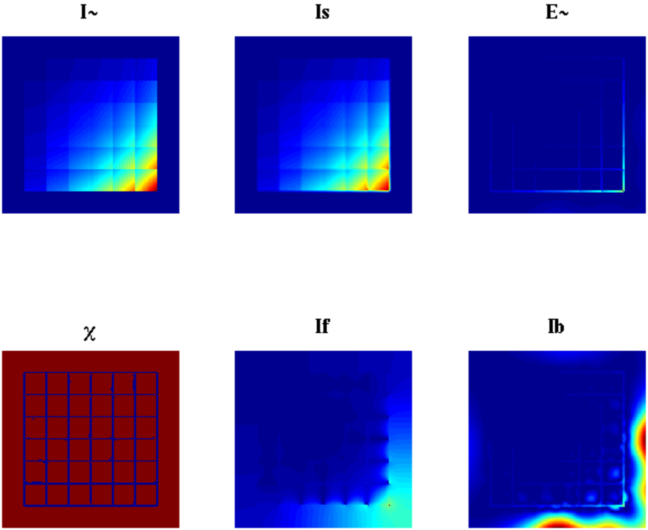

Computational Investigation of the Approach

2D Examples:

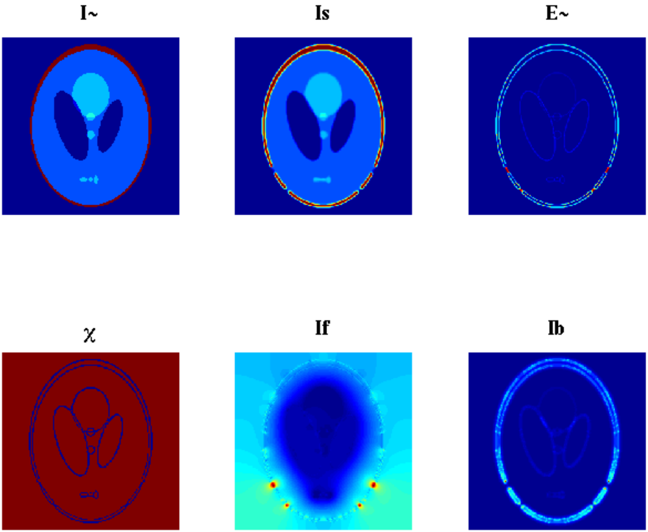

Obtaining a Segmentation

With χ in hand, the multiphase approach can be well initialized. For the above examples:

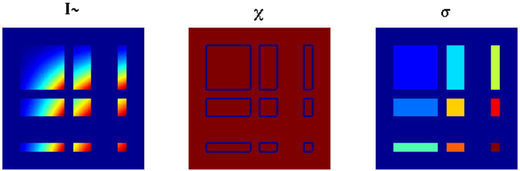

Obtaining a Segmentation

With χ in hand, the multiphase approach can be well initialized.
For the above examples:

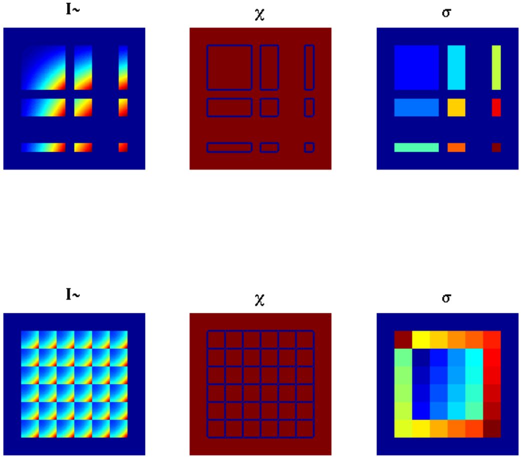

Defining a Segmentation

With χ in hand, the multiphase approach can be well initialized.
For the above examples:

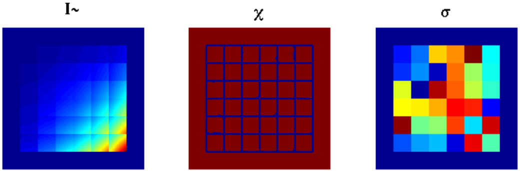

Defining a Segmentation

With χ in hand, the multiphase approach can be well initialized. For the above examples:

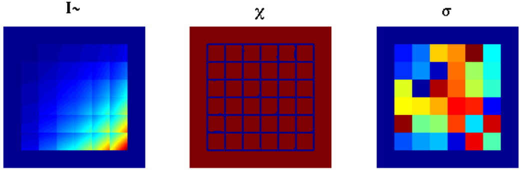

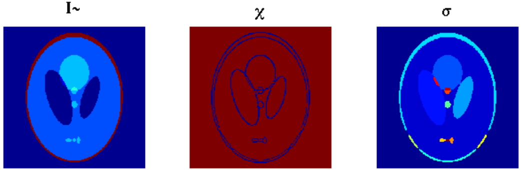

Application to Measured Images

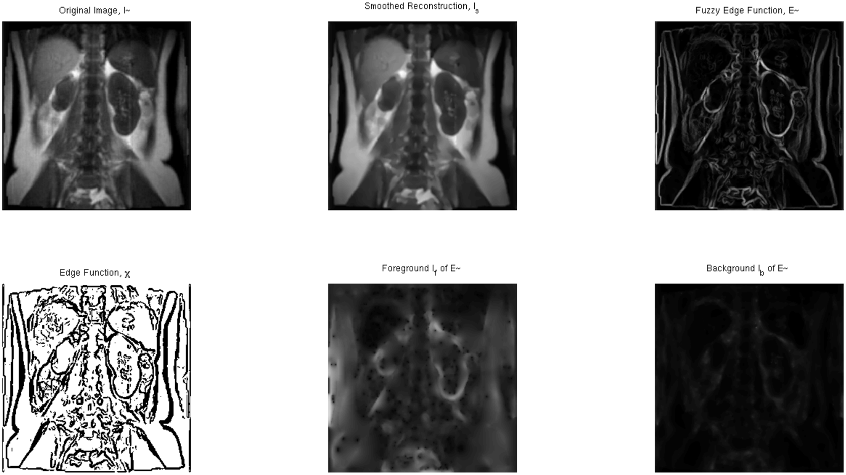

Application to Measured Images

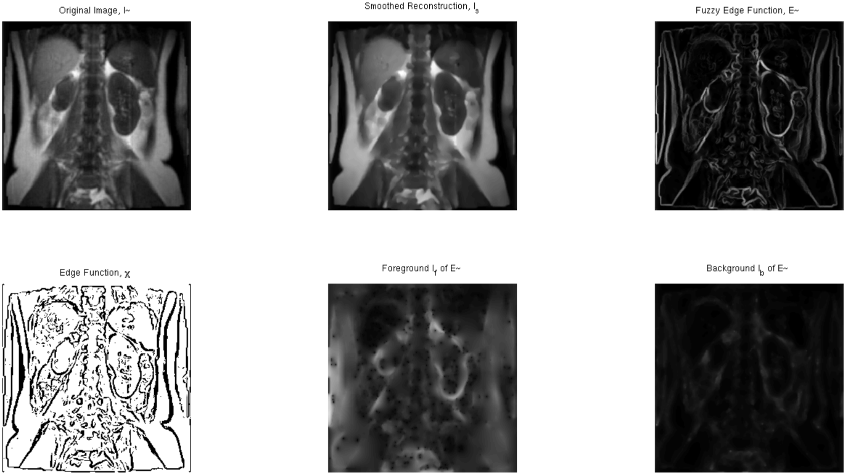

Application to Measured Images

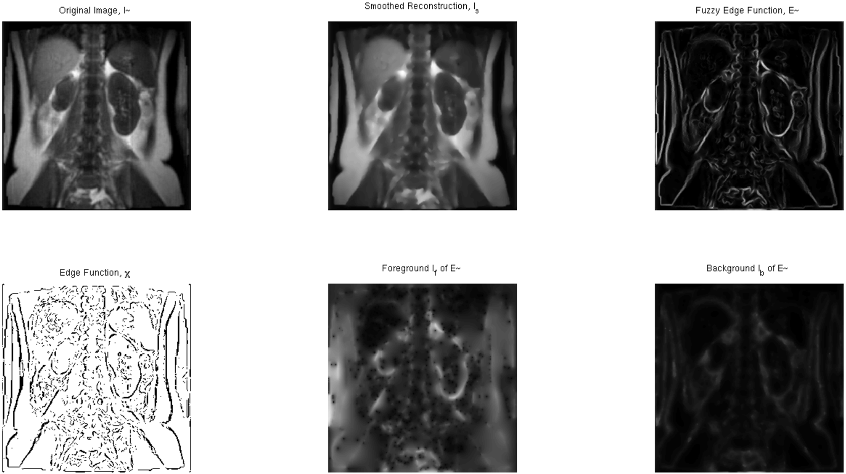

Application to Measured Images

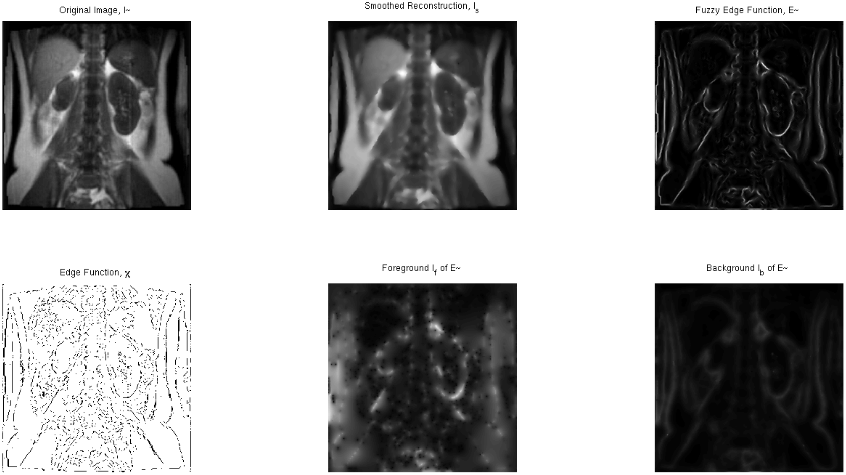

Application to Measured Images

Comparison of the fuzzy edge function

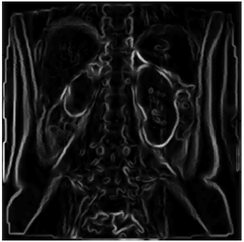

Application to Measured Images

Comparison of the fuzzy edge function with a higher order Ambrosio-Tortorelli approach:

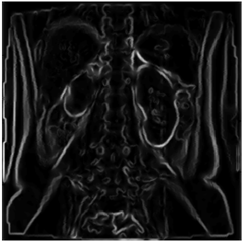 

Application to Measured Images

Comparison of the fuzzy edge function with a higher order Ambrosio-Tortorelli approach:

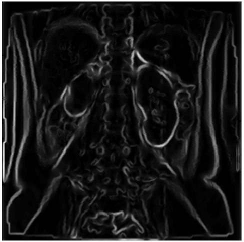


and the respective edge functions,


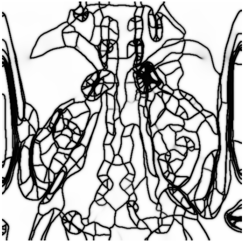

Application to Measured Images

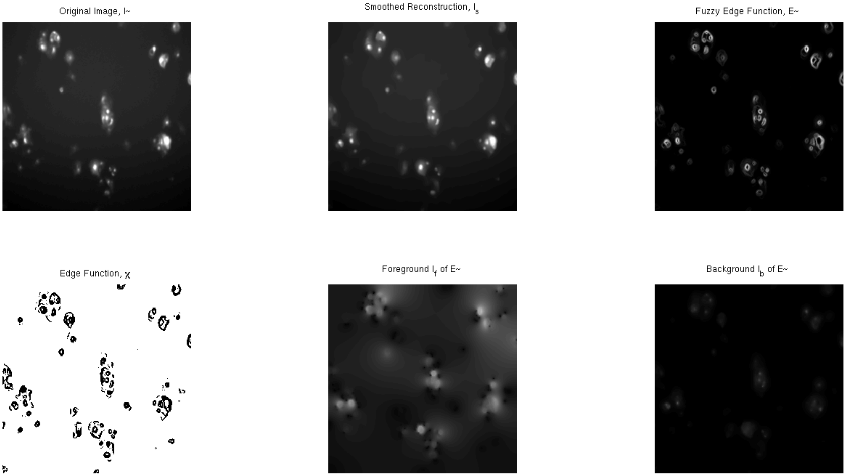

Application to Measured Images

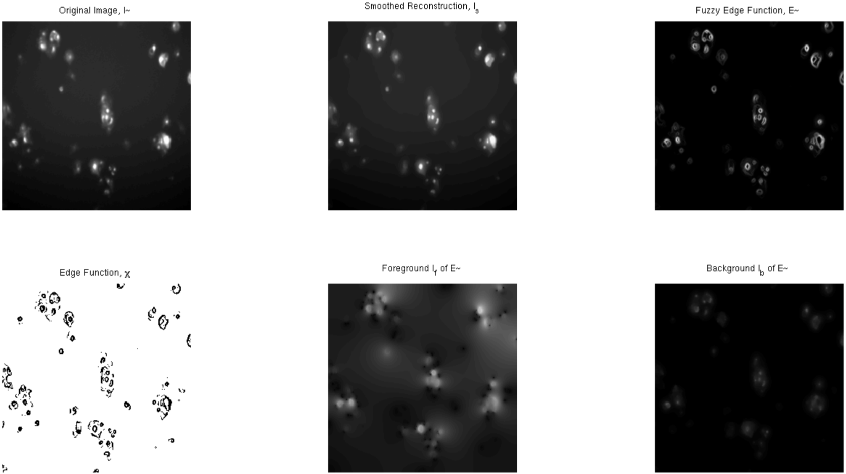

Application to Measured Images

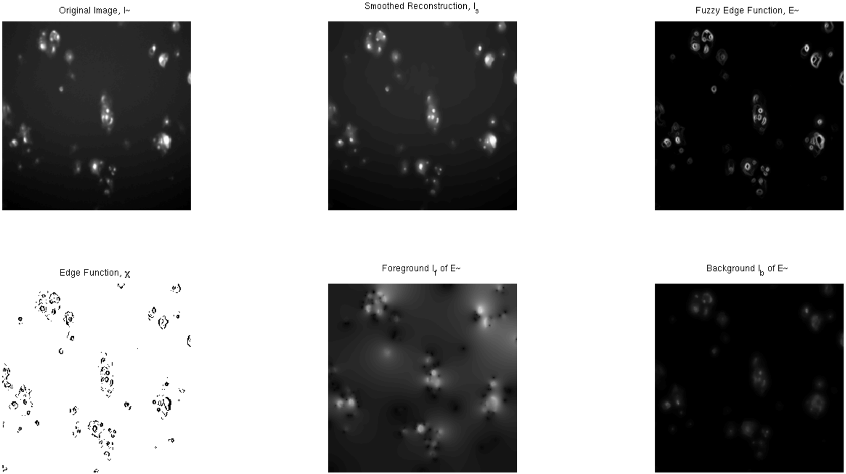

Application to Measured Images

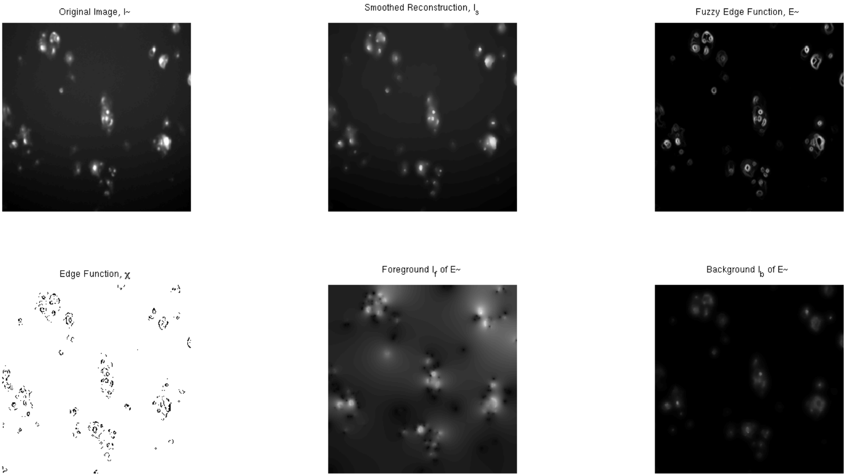

Registration of Edge Sets

For mapping a Purkinje fiber network system [Fürtinger & Keeling]:

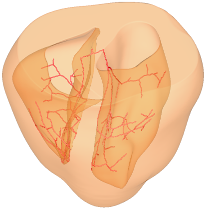

Registration of Edge Sets

For mapping a Purkinje fiber network system [Fürtinger & Keeling]:

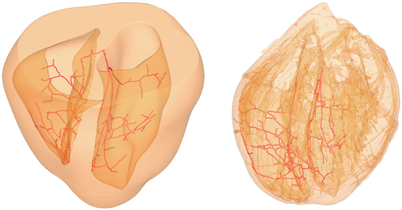

Performed using 2D slices,

$$\min_{\boldsymbol{u}} \int_{\Omega} \left\{ |I_0^\epsilon \circ (\mathrm{Id} + \boldsymbol{u}) - I_1^\epsilon|^2 + \mu |\nabla \boldsymbol{u}^{\mathrm{T}} + \nabla \boldsymbol{u}|^2 \right\}$$

Registration of Edge Sets

For mapping a Purkinje fiber network system
[Fürtinger & Keeling]:

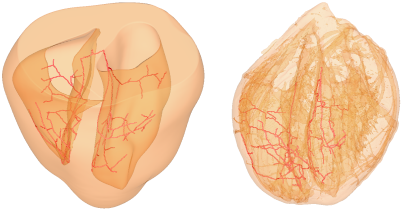

Performed using 2D slices,

$$\min_{\boldsymbol{u}} \int_{\Omega} \left\{ |I_0^\epsilon \circ (\mathrm{Id} + \boldsymbol{u}) - I_1^\epsilon|^2 + \mu |\nabla \boldsymbol{u}^{\mathrm{T}} + \nabla \boldsymbol{u}|^2 \right\}$$

with diffuse images I_0^ϵ and I_1^ϵ, providing strong registration force, then $\epsilon \to 0$.

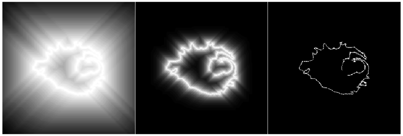

Registration of Edge Sets

But reducing $\epsilon \to 0 \Rightarrow \text{argmin} = 0$! Landscape is

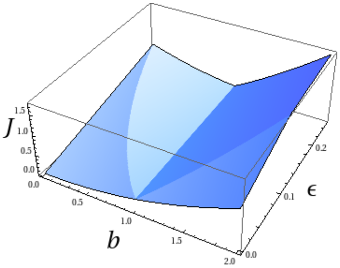

Registration of Edge Sets

But reducing $\epsilon \to 0 \Rightarrow \text{argmin} = 0$! Landscape is

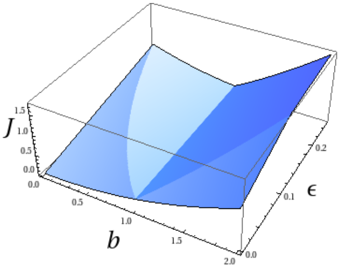

Theorem: There exists a minimizer $\boldsymbol{u}^{\epsilon} \in H^1(\Omega)$ which converges (subsequentially) in $H^1(\Omega)$ as $\epsilon \to 0$.

Registration of Edge Sets

But reducing $\epsilon \to 0 \Rightarrow \text{argmin} = 0$! Landscape is (@ left)

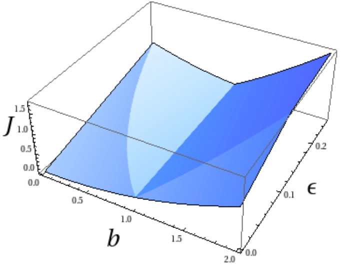

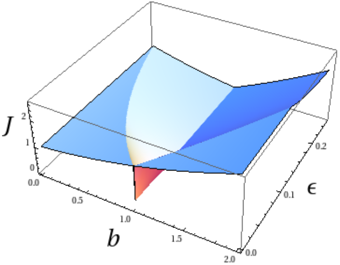

Theorem: There exists a minimizer $\boldsymbol{u}^\epsilon \in H^1(\Omega)$ which converges (subsequentially) in $H^1(\Omega)$ as $\epsilon \to 0$.

However, with

$$\int_\Omega |I_0^\epsilon \circ (\mathrm{Id} + \boldsymbol{u}) - I_1^\epsilon|^2 \quad \to \quad \int_\Omega |I_0^\epsilon \circ (\mathrm{Id} + \boldsymbol{u}) - I_1^\epsilon|^2 \Big/ \int_\Omega [|I_0^\epsilon|^2 + |I_1^\epsilon|^2]$$

the landscape becomes (@ right).

Registration of Edge Sets

But reducing $\epsilon \to 0 \Rightarrow \text{argmin} = 0$! Landscape is (@ left)

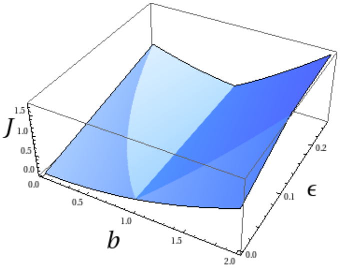

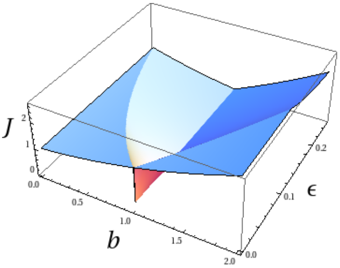

Theorem: There exists a minimizer $\boldsymbol{u}^\epsilon \in H^1(\Omega)$ which converges (subsequentially) in $H^1(\Omega)$ as $\epsilon \to 0$.

However, with

$$\int_\Omega |I_0^\epsilon \circ (\mathrm{Id} + \boldsymbol{u}) - I_1^\epsilon|^2 \quad \to \quad \int_\Omega |I_0^\epsilon \circ (\mathrm{Id} + \boldsymbol{u}) - I_1^\epsilon|^2 \Big/ \int_\Omega [|I_0^\epsilon|^2 + I_1^\epsilon|^2]$$

the landscape becomes (@ right).

Convergence to Hausdorf distance between edge sets to be shown.

Thank You!